



Ring closing metathesis by Hoveyda–Grubbs catalysts: A theoretical approach of some aspects of the initiation mechanism and the influence of solvent



Égil de Brito Sá^{a,b}, José Milton Elias de Matos^{b,*}

^a Laboratório Interdisciplinar de Materiais Avançados, Centro de Ciências da Natureza, Federal University of Piauí, 64049-505, Ininga, Teresina, PI, Brazil

^b Campus of Parnaíba, Federal University of Piauí, 64202-020, Parnaíba, PI, Brazil

ARTICLE INFO

Article history:

Received 1 May 2014

Received in revised form 10 November 2014

Accepted 15 November 2014

Available online 25 November 2014

Keywords:

Olefin Metathesis

Solvent Influence

DFT

Mechanism of Initiation

Monte Carlo Simulation

Hoveyda–Grubbs Catalyst

ABSTRACT

Olefin metathesis is a type of chemical reaction with a wide range of applications. Despite intense study, the mechanism of this reaction and the effects of solvent are still poorly understood. The full RCM catalytic cycle of N-tosylallylamine and a Hoveyda–Grubbs catalyst were examined using density functional theory. We considered two different possibilities for the initiation step, and the pathway that included interconversion of the 14 electron structure was found to be the most stable. Important solvent influences were revealed using the PCM method, as the reaction was found to be much more favourable in all of the solvents studied herein. We did not detect any significant differences between the solvents considered by this approach, but we did find that dichloromethane and methanol are better than water for this reaction, as was expected. Classical Monte Carlo simulations of the solvation process revealed that water is a poor solvent, but solvation became better with addition of methanol. Also, the Monte Carlo simulations showed that dichloromethane is the best solvent of those analysed followed very closely by methanol.

© 2014 Published by Elsevier B.V.

1. Introduction

Catalysed olefin metathesis reactions are an important method to form a carbon–carbon double bond (C=C) even in the presence of other functional groups [1]. This reaction involves an apparent interchange of carbon atoms between two pairs of double bonds. The result is that each half of one olefin molecule is bound to half of a second olefin [2]. This method is a powerful tool in organic synthesis and polymer chemistry, and is mainly applied in one of three ways: Ring Opening Metathesis Polymerisation [3], Cross Metathesis [3,4] and, importantly, Ring Closing Metathesis (RCM) [5]. RCM is particularly useful in pharmaceutical applications. The most widely accepted mechanism for the reaction, proposed by Chauvin and Herrissón, consists of a series of formal cycloadditions and cycloreversions involving: olefin coordination to a transition metal carbene (M=C) complex to form a π complex, migratory insertion of the olefin ligand into the M=C bond to yield

a metallocyclobutane, breaking of two different bonds to form another π complex, and dissociation to give the products [6].

The rise of the metathesis reaction occurred as “well-defined” catalysts composed of early-transition-metal carbenes were developed, as shown in Fig. 1. The first metal carbenes were synthesised with W and Mo by Schrock (**1a**). Prior to these catalysts, the applications of metathesis reactions were limited because the metal centres are oxophilic and electrophilic, making them sensitive to air, moisture and reactive functional groups [7]. The development of Ru-based complexes by Grubbs and co-workers further popularised the reaction. These complexes, commonly referred to as the first, (**1b**) [(PCy₃)₂Cl₂Ru = CHPh], and second, (**1c**) [(H₂IMes)(PCy₃)Cl₂Ru = CHPh], generation Grubbs catalysts, were successfully used in the metathesis of a number of different olefins, such as strained and low-strain cyclic olefins, exocyclic olefins, and straight-chain alkenes [8]. A fourth type of catalyst, stable ruthenacarbenes derived from Grubbs type complexes, were first reported by Hoveyda and co-workers and were aptly named Hoveyda–Grubbs catalysts. In these catalysts the benzylidene and PCy₃ are replaced with a bidentate benzylidene ether ligand, which displays excellent thermal stability and oxygen- and moisture-tolerance [9,10].

The use of water as a solvent offers several advantages, such as safety, economy, and environmental compatibility. However, like

* Corresponding author at: Campus Universitário Ministro Petrônio Portella – Bairro Ininga, Centro de Ciências da Natureza – CCN, Departamento de Química, CEP: 64.049-550 Teresina – PI, Brazil. Tel.: +55 86 3215 5840; fax: +55 86 3221 5710.

E-mail address: jmematos@ufpi.edu.br (J.M.E. de Matos).

other organic reactions, olefin metathesis is carried out almost exclusively in aprotic, dry and degassed organic solvents under a protective inert atmosphere [1,11]. There are several explanations given for this behaviour; some authors say that the well-defined catalysts, like other organometallic systems, are oxygen and functional group sensitive. Thus, carrying out the reactions in organic solvents is necessary to avoid catalysts deactivation by oxygen and moisture [12,13]. Others have published found that some well-defined catalysts are stable and active in the presence of polar and protic moieties, such as alcohols, aldehydes, ketones, carboxylic acids, esters, amides, and water. Although these catalysts are active in the presence of protic solvents such as water and methanol and water, they are insoluble in these solvents. In this way, the main challenge is finding catalysts and olefins that are soluble in water or other polar and protic solvents [14–17].

The development of aqueous reaction conditions suitable for water-insoluble substrates and catalysts may be the simplest solution to this problem. Bleichert and co-workers [13] reported a possible alternative: carry out homogenous metathesis in aqueous media with co-solvents. Using catalysts **1c** and **1d** in water-methanol and water-DMF mixtures, they found high conversion of N-tosyldiallylamine by RCM in a reaction time of 12 h. This could be partially due the solubility of the pre-catalysts in aqueous solvent allowing improved contact with the substrate. Based on these studies, the aim of this paper is to use theoretical efforts to understand the influence of aqueous solvents on the RCM of N-tosyldiallylamine with catalyst **1d**, specifically focusing on the solubility of the systems. To the best of our knowledge, there are no systematic theoretical efforts to understand the influence of solvent in metathesis reactions.

Another aim of this work is gain detailed information about the initiation step of the reaction mechanism. Understanding this part of the mechanism is very important because it is central to understanding the entire catalytic cycle. Despite many theoretical efforts on Grubbs catalysts, to our knowledge, only three works have described the metathesis with Hoveyda–Grubbs catalyst: two of them use a dissociative mechanism [18,19] and the other uses an interchange-associative mechanism [20]. We found that the mechanism of catalysis depends on the size of both the olefin and the Hoveyda ligand. This result agreed with experimental publications, where the mechanism also depends of the olefin and Hoveyda ligand size [21]. In fact, the exact initiation mechanism still remains unclear.

2. Computational methods

One purpose of this work is to explore the potential energy surface (PES) in the gas phase for the Ring Closing Metathesis reaction of N-tosyldiallylamine using a second generation Hoveyda–Grubbs catalyst. All quantum chemical calculations were performed using Density Functional Theory developed by Khon-Shan [22]. The geometries of the reactants, products, intermediates and transition states were optimised using Becke's hybrid exchange functional with three parameters (B3) [23] and the correlation functional from Lee, Yang, and Parr (LYP) [24]. All atoms were represented using the Pople's basis set 6-31g(d) [25] except for the ruthenium, which was described using LanL2DZ. This approach treats the inner

electrons as the core potential described by Hay and Wadt [26]. The stationary points in the PES were characterised by vibrational frequency calculations conducted using the same level of theory. In these calculations, a structure is considered a minimum if it has neither an imaginary frequency nor a transition state and if it presents only one structure. The structures of the PES for this reaction were based on a theoretical study of a similar reaction [18]. A key difference, though is that this previous publication treated the structures as models to simplify the calculations, and in our work we present their real structures. Discussion of the energy profile for the reaction is based on the Total Electron Energy relative to the reagents of each part of the cycle (ΔE).

Another important goal of this work is to evaluate the effect of solvents on the reaction. To consider the influence of different solvents, we used the Polarizable Continuum Method (PCM) [27], during which single-point calculations were performed on all gas phase optimised structures. In the PCM model, the solvent is considered as a continuous dielectric and is defined by a dielectric constant. We considered the effects of six different solvents: water ($\epsilon = 78.35$), dichloromethane ($\epsilon = 8.93$), methanol ($\epsilon = 32.61$) and three water–methanol mixtures: 3:1 ($\epsilon = 65.55$), 1:1 ($\epsilon = 56.28$) and 1:3 ($\epsilon = 45.24$). The dielectric constants representing the solvents mixtures were obtained experimentally [28]. The UAHF [29] model was used for the generation of the cavity. These solvents were also used in the experiments to evaluate their effects on the homogeneous reaction of N-tosyldiallylamine using a Hoveyda–Grubbs catalyst [13]. Despite the fact that real solvent is defined by other parameters besides the dielectric constant, the PCM has been used efficiently to study organometallic catalytic processes [30], including olefin metathesis [31]. For example, Cavallo et al. recently studied the influence of some solvents on the initiation stage of the catalytic cycle for an RCM reaction [32]. The influence of the different solvents on the catalytic cycle was considered by considering the Free Energy of Solvation (ΔG_{solv}) of each of the species in addition to its total electronic energy ($E_{\text{gas}} + \Delta G_{\text{solv}}$). This approach is often used in studies of organometallic catalysis, particularly with olefin metathesis [31]. Another possibility would be to use ($G_{\text{gas}} + \Delta G_{\text{solv}}$), but this oversimplification ignores entropic contributions to the Gibbs free energy that occur when the molecularity changes. When we use $E_{\text{gas}} + \Delta G_{\text{solv}}$, some of the entropy is considered in ΔG_{solv} , which compensates for the error in considering only the total electronic energy (E_{gas}).

Monte Carlo simulations are another methodology that can also be used to evaluate the effect of solvent. In this work, we have evaluated the interactions between the different solvents and both the Hoveyda–Grubbs catalyst and the substrate of the reaction, N-tosyldiallylamine. Six solvent simulations were performed for the catalyst and six for the olefin, one each for water, methanol, dichloromethane, water–methanol 3:1, water–methanol 1:1 and water–methanol 1:3. We used standard procedures, including the Metropolis sampling technique, the canonical NVT ensemble and periodic conditions of contour using the method of images in a cubic box generated from the experimentally determined density of the solvent [33]. All simulations were performed at $T = 298.15$ K with one molecule of solute (catalyst or olefin) surrounded by 1000 molecules of solvent. The characteristics of all simulations are in Table 1.

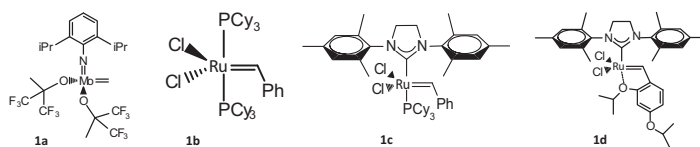


Fig. 1. Evolution of the main olefin metathesis catalysts.

Table 1
Composition of solvents for Monte Carlo simulation.

Solvent	Density (g cm ⁻³)	Size of the side box (Å)	Solvent composition (nmol)		
			Water	Methanol	Dichloromethane
Water	0,997	[‡] 31,46; [‡] 31,21	1000	0	0
Water–Methanol 3/1	0,930	[‡] 34,10; [‡] 33,87	750	250	0
Water–Methanol 1/1	0,875	[‡] 36,54; [‡] 36,33	500	500	0
Water–Methanol 1/3	0,829	[‡] 38,13; [‡] 38,63	250	750	0
Methanol	0,787	[‡] 41,02; [‡] 40,84	0	1000	0
Dichloromethane	1,327	[‡] 47,49; [‡] 47,41	0	0	1000

[‡] Hoveyda–Grubbs catalyst.

[‡] N-tosyldiallylamine.

The molecular interactions are described by the sum of the Lennard-Jones and Coulombic potentials:

$$U_{ab} = \sum_i^a \sum_j^b 4\epsilon_{ij} \left[\left(\frac{\sigma_{ij}}{r_{ij}} \right)^{12} - \left(\frac{\sigma_{ij}}{r_{ij}} \right)^6 \right] + \frac{q_i q_j}{r_{ij}}$$

where \sum^a is the sum over all of the atoms of molecule *a* and \sum^b is the sum over all of the atoms of molecules *b*, $\epsilon_{ij} = \sqrt{\epsilon_i \epsilon_j}$, $\sigma_{ij} = \sqrt{\sigma_i \sigma_j}$ are the Lennard-Jones parameters and *q* is the partial charge of each atom.

The structure of the catalysts and of the olefin were determined by optimisation at the B3LYP/6-31g(d) theoretical level, and the partial atomic charges were calculated using the ChelpG [34] procedure at the same level. For the Lennard-Jones parameters, the OPLS force field was used [35] for all atoms except ruthenium, which we modelled with the UFF potential as suggested by Rocha co-workers [36]. The OPLS force field was also used to obtain the geometries, Lennard-Jones parameters and atomic charge of methanol [37] and dichloromethane [38]; for the water, we used the model TIP3P [39]. A new configuration of solvent is generated after 1000 Monte Carlo steps. All simulation are composed of an initial stage of thermalisation with 5×10^7 steps and an equilibration phase of 1×10^8 steps. The properties are evaluated only during the equilibration phase.

The calculations of the catalytic cycle in the gas-phase and the evaluation of the effect of the solvent via PCM were performed using the GAUSSIAN 09 package of programs [40] and Monte Carlo simulations using the DICE program [41].

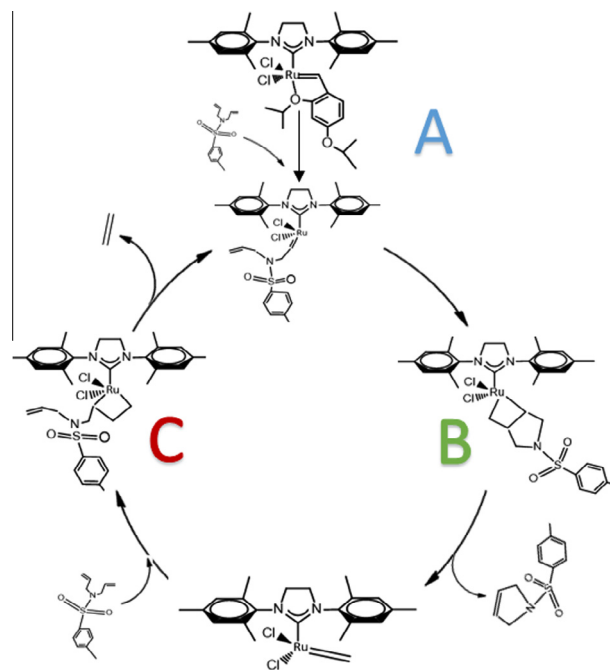
3. Results and discussion

We present the results as follows: a discussion of some relevant aspects of the gas phase catalytic cycle, a presentation of the solvent influence results determined using the PCM, and finally, an analysis of the results of the Monte Carlo simulations.

3.1. Gas-phase catalytic cycle

The entire catalytic cycle is shown in Scheme 1. The mechanism is based on three main parts: activation and initiation (part A), a cross metathesis reaction with the first double bond of the olefin (part B) and the reaction of the second double bond of the olefin (part C), which results in ring closing.

There are many theoretical works for the first and second generation Grubbs catalysts [31], and it is well established that the activation process occurs through a dissociative mechanism. For the Hoveyda–Grubbs catalyst, however, there are few publications, and there is not a consensus on the mechanism. Here, we will adopt the dissociative mechanism due to the size of the olefin molecule, which would very difficult to undergo an associative mechanism of activation, as shown in other publication [18]. Also, we explore two paths for the initiation process, shown in Fig. 2, that also presents the PES for this part of our study.



Scheme 1. General scheme for the mechanism of RCM of the N-tosyldiallylamine with a Hoveyda–Grubbs catalyst.

Before entry into one of the two possible paths, referred to herein as **I** and **II**, activation starts with the pre-catalyst **A1**. The calculated structure of **A1** is discussed in the first part of [Supporting Information](#). The next step involves the dissociation of the isopropoxide fragment of the Hoveyda ligand. This process involves a transition state, **TS (A1–A2)**, which has an energy that is 19.33 kcal mol⁻¹ greater than the reagents. In this transition state, the oxygen O1 that was only 2.38 Å from the Ru atom moved to 3.58 Å away, suggesting that in this transition state, the Ru···O interaction no longer exists. The structure with minimal energy that drives the transition through this state is the species **A2**, whose structure is shown in Fig. 3. In this structure, the Hoveyda ligand has been completely removed with a Ru···O distance of 4.5 Å. This species, having 14 electrons around the metal centre and a vacant site for complexation with the incoming olefin, is of fundamental importance for the metathesis reaction because it allows the interaction of the catalyst with the olefin. Species **A2** is 8.72 kcal mol⁻¹ more stable than the transition state. Once species **A2** is formed, the two paths of initiation, **I** and **II**, begin. Path **I** (shown in Part A of Scheme 1), progresses via the introduction of the olefin (**O**) into the catalytic cycle. **O** then interacts with species **A2** by cycloaddition [2+2], resulting in the formation of a π-complex corresponding to the **LA3** structure.

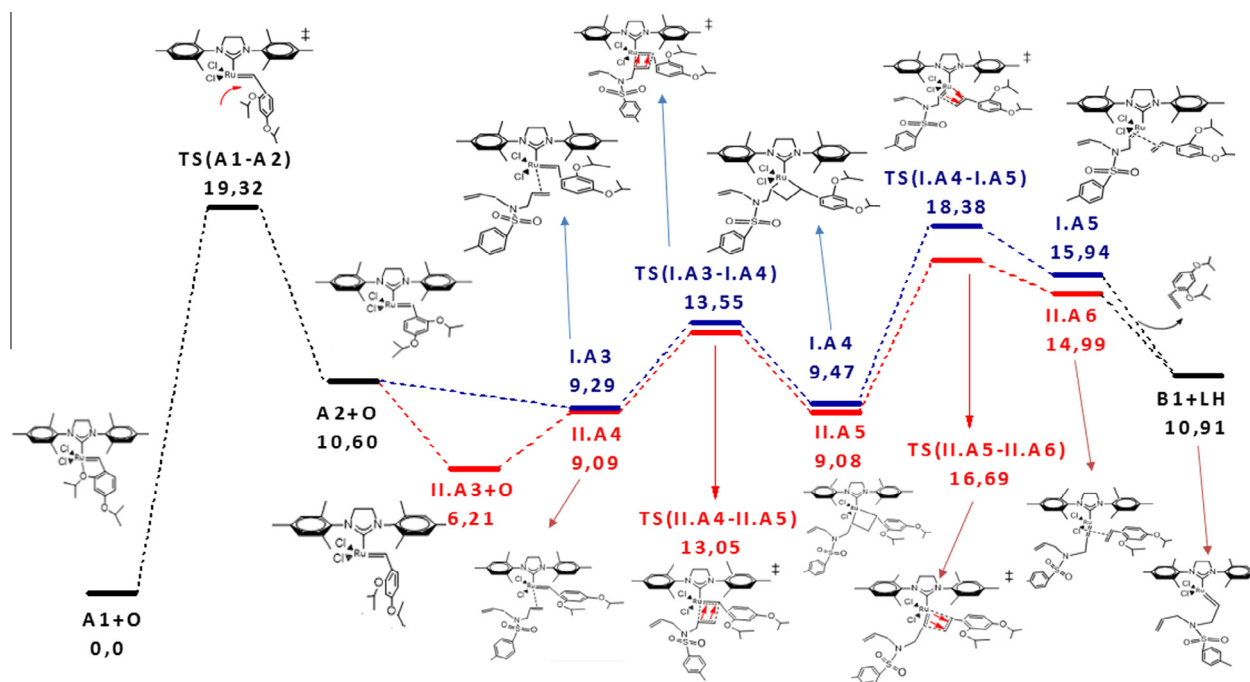


Fig. 2. PES (total electronic energy in kcal mol⁻¹) for the catalyst activation process and initiation of RCM.

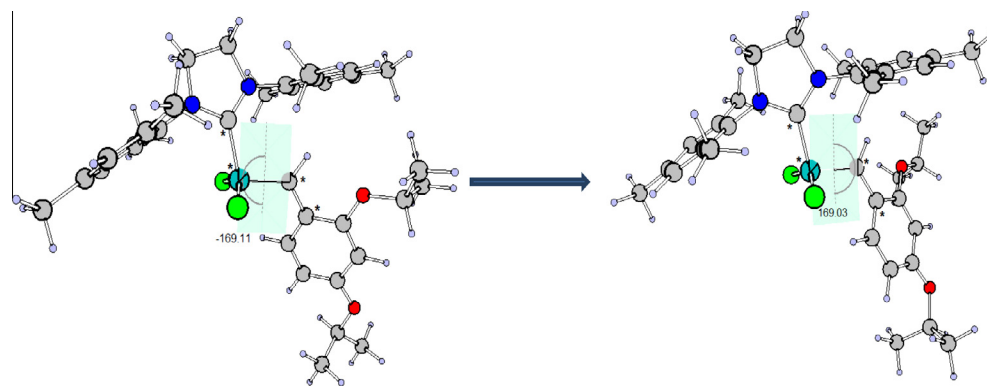


Fig. 3. Interconversion of catalyst with vacant site. Distances Ru=C in Å and dihedral angles in degrees (°). Atoms forming the dihedral angles are marked with asterisk.

Path **II** is also in Fig. 2. This path also begins with the catalyst **A1**, passes through the transition state **TS (A1–A2)** and arrives at structure **A2**. While path **I** involves the immediate coordination of the olefin and creation of the **I.A3**, path **II** involves no complexation of the olefin. Rather, a rotation through the Ru=C bond is utilised, resulting in the structure **II.A3** shown in Fig. 3.

Structure **II.A3** has a dihedral angle of $-169,11^\circ$ between the carbon of the coordinated mesityl group, the ruthenium atom, the carbene carbon and the carbon of the aryl group bound to the carbene, $\text{NCN}^{\text{r}}\text{—Ru=C—C}_{\text{aryl}}$ (marked with asterisk in Fig. 2). In contrast, structure **A2** has a dihedral angle of $169,3^\circ$, demonstrating the rotation of the entire Hoveyda group around the connecting Ru=C. This rotation occurs easily and has already been shown in other theoretical and experimental studies [42]. In path **II**, the Ru=C bond length is kept constant (1.856 Å in **A2** and 1.857 Å in **II.A3**); meanwhile, the length of the Ru...O bond in **II.A3** is 4.51 Å and in **A2** is 4.50 Å, suggesting that this interaction is unchanged. Interconversion is governed by energy, and will be discussed later. The structure **II.A3** is $4.39 \text{ kcal mol}^{-1}$ more stable than its isomer **A2**. Using the PES, complexation of the olefin to

the catalyst's vacant site in **II.A3** forms the structure **II.A4**; this event is also a cycloaddition [2+2] process.

Analysing the PES of the two paths, we see that there is no significant difference between the paths **I** and **II**; however, we believe that path **II** is more plausible because the interconversion process is more favourable and may happen before the olefin coordination that would lead to path **I**. Moreover, path **II** is more favourable than path **I** according to the PES, though this difference is within the experimental error (see Fig. 2). The remaining steps take place without any major energy barriers, so the reaction would occur without any major problems for both paths. However, it is interesting to note that the products of the initiation step are endergonic, and have energies that are $10.9 \text{ kcal mol}^{-1}$ higher than the reagents according to the PES.

So far, we have described only initiation of the reaction. After forming **A6 = B1**, the productive reaction occurs by a rearrangement of the structures, leading to the coordination of the second π -bond by an intramolecular cycloaddition [2+2] process to the metallic centre, which would create the structure **B2**. This part of the mechanism involves closing the olefin. Part B of Scheme 1 is

the real turnover catalytic cycle. Fig. 4 shows the PES for this part of the reaction together with the structures.

Thus far, we have discussed the RCM process beginning with the catalyst **A1**, which is actually a pre-catalyst that exists in the reaction mixture at average levels from 0.5% to 5% of the total olefin [1]. Thus, there are not as many molecules of pre-catalyst as there are of olefin, suggesting that the species responsible for propagation of the reaction (i.e., consumption of all of the olefin molecules) is **B5 = C1**. After all of the olefin is consumed, the pre-catalyst is regenerated. Then, turnover of this reaction occurs at each cycle through the stages of part C, ending with a molecule of ethylene (**E**) and an active species, the metal carbene **B1**. The reaction then continues with Part B in the cycle of Scheme 1. In Fig. 5, we show the PES for the whole turnover of the catalytic cycle.

In the propagation reaction, π -complex formation, species **C2**, is favourable unlike what occurs during the activation of **A1** because the metalcarbene group in **C1** is smaller than in **IA3**. Thus, sterics are very important to this complexation, which also suggests that the use of models is insufficient for good descriptions of reactions. Another important point is the great stability of the metallocyclobutane **C3** relative to the other metallocycles from other steps. This increased stability implies that there is a large barrier to opening the metallocycle to produce the products **B1** and **E**. Once **B1** is formed, the reaction follows the same path discussed previously. The products of the gas phase reaction (**B5 + P + E**) have much higher energy ($12.11 \text{ kcal mol}^{-1}$) than the reagents (**C1 + P**).

3.2. Influence of the solvent determined via PCM

Tables 2 and 3 shows the influence of various solvents on olefin metathesis. The corrections for solvent were made by adding the free energy of solvation (ΔG_{solv}) to the energy of the gas phase. Table 2 shows the results for the initiation step by Path **IIA**, which was found to be the most energetically favourable, and the contribution of solvent on Part B, completing the mechanism for the cyclisation of the first olefin.

Since the main effects of all of the examined solvents were similar, we will discuss dichloromethane, the standard solvent used for this reaction. There is a general stabilisation throughout the catalytic cycle; lower energies, especially the stabilisation of the

14 electron species **A2** and **IIA.3**, are observed. Formation of the π -complexes in **IIA.4** is also much more favourable in solution than in the gas phase. Other species that are stabilised substantially are the products of the catalytic cycle, the carbene **B5** and the olefin **P**. This increased stability is due to the entropy of the separated products, as entropy is partially taken into account by incorporating the free energy of solvation [18–21]. When including the solvent effects, the π -complex formed after breaking the metallocyclobutane, **IIA.6**, is no longer an energy minimum in the PES. Therefore, is not a species of the catalytic cycle, despite having a value in Table 2. This result suggests that in solvent, opening the metallocyclobutane goes through a transition state that leads the reaction directly to the products. However, the π -complex **B4** is still a minimum from the PES even in solvent, indicating that formation of products is favourable. The formation of products, in general, becomes more favourable, as the products in the gas phase are $19.20 \text{ kcal mol}^{-1}$ higher than the reactants in energy, whereas in dichloromethane this difference is only $12.68 \text{ kcal mol}^{-1}$.

In Table 3, we present the energy of solvation for the turnover of the reaction. The same consideration made above can be made to cycle of turnover. It is interesting to note the high stability of the π -complex formation relative to the gas phase and the considerable stability conferred by the solvent to the products such that the products are practically isoenergetic to the reagents ($0.77 \text{ kcal mol}^{-1}$ in dichloromethane). In the gas phase, this value was $12.11 \text{ kcal mol}^{-1}$. This increased stability is due to the free energy of solvation, which takes entropy into account. Here, the π -complexes formed after the opening of the metallocycle are no longer minima in the PES.

Dichloromethane's superior ability to stabilise the π -complexes **C2** and **IIA.4** over water indicates that metathesis occurs more easily in dichloromethane because of better solubility of both the catalyst and the olefin. Methanol had an intermediate value between water and dichloromethane for the complex formation, which justifies the intermediate yield of reaction conducted in methanol. However, these values are not significant enough to justify the differences in experimental yield. As to other values along the catalytic cycle, there are no significant differences. At this level of theory, PCM methodology was not capable of showing significant differences between the mixtures of water and methanol despite experimentally observed differences between them.

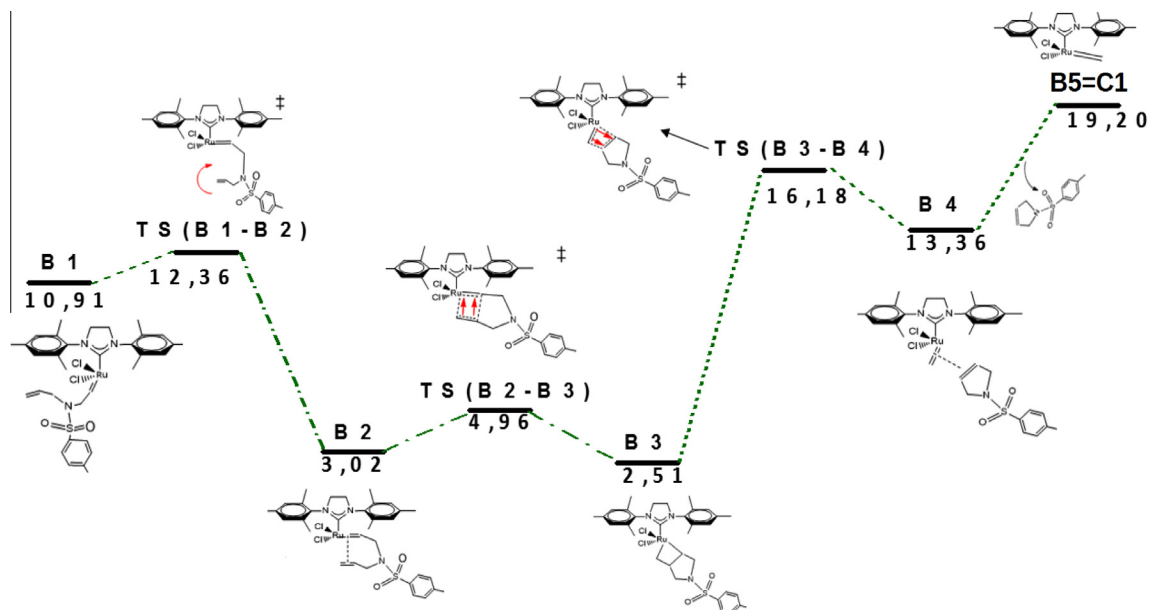


Fig. 4. Energy profile of Part B of RCM.

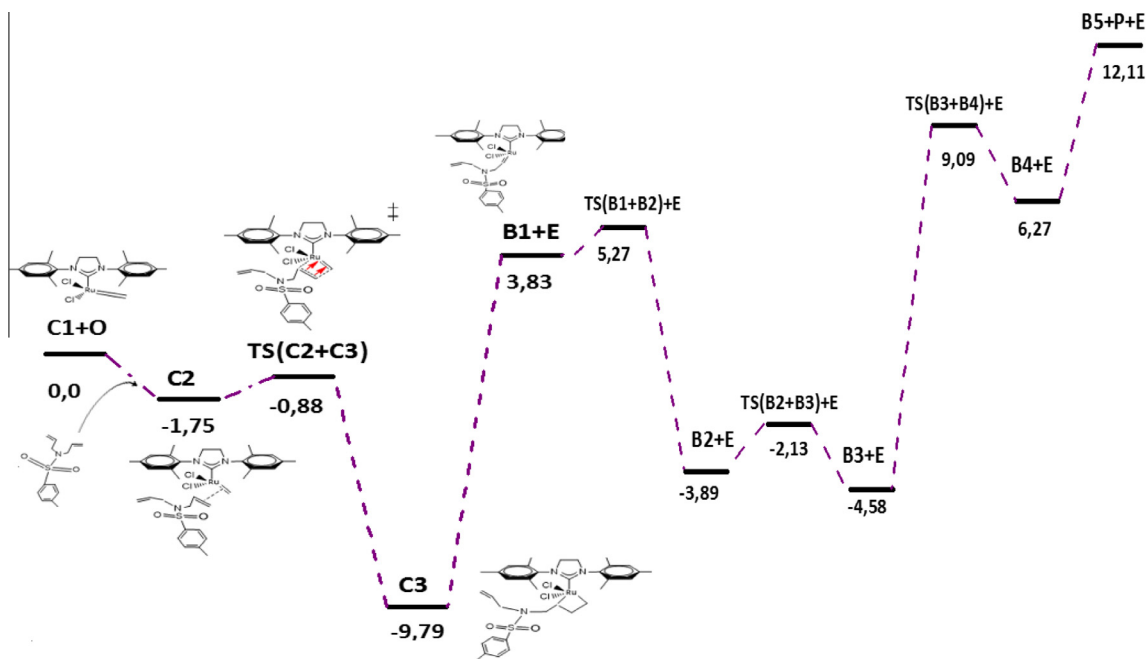


Fig. 5. Profile of energy of the propagation cycle of the RCM of the N-tosylallylamine starting as active catalyst C1.

Table 2

The gas phase energy and in different solvents for the cyclization of the first olefin.

Stationary point	Gás phase	CH ₂ Cl ₂	H ₂ O	H ₂ O/MeOH			MeOH
				3:1	1:1	1:3	
1 + O	0,0	0	0	0	0	0	0
TS(A1–A2) + O	19,32	18,17	17,84	17,85	17,86	17,88	17,92
A2 + O	10,60	8,06	7,48	7,51	7,53	7,55	7,61
II.A3 + O	6,21	3,53	2,92	2,94	2,97	2,99	3,06
II.A4	9,09	3,63	4,60	4,58	4,56	4,51	4,43
TS (II.A4–II.A.5)	13,05	8,66	9,54	9,53	9,52	9,48	9,42
II.A5	9,08	2,99	3,14	3,16	3,17	3,18	3,20
TS (II.A5–II.A.6)	16,69	8,55	8,06	8,09	8,12	8,16	8,24
II.A6	14,99	8,98	9,20	9,20	9,21	9,21	9,22
B1 + LH	10,91	7,19	8,06	7,02	7,32	6,51	7,05
TS(B1–B2) + LH	12,36	8,68	9,19	8,50	8,80	7,99	8,54
B2 + LH	3,02	1,88	3,45	2,72	2,99	2,13	2,57
TS(B2–B3) + LH	4,96	3,58	4,97	4,25	4,53	3,66	4,12
B3 + LH	2,51	2,79	4,47	3,74	4,01	3,13	3,56
TS(B3–B4) + LH	16,18	14,27	15,20	14,50	14,79	13,96	14,46
B4 + LH	13,36	12,33	13,55	12,84	13,12	12,27	12,74
B5 + P	19,20	12,68	13,01	12,37	12,64	11,83	13,67

Table 3

Energy in the gas phase and in different solvents for the cycle turnover.

Stationary point	Gás phase	CH ₂ Cl ₂	H ₂ O	H ₂ O/MeOH			
				3:1			
C1 + O	0,0	0	0	0	0	0	0
C2	-1,75	-7,40	-6,65	-6,62	-6,69	-6,69	-6,75
TS(C2 + C3)	-0,88	-6,15	-5,29	-5,28	-5,36	-5,35	-5,43
C3	-9,79	-13,72	-12,65	-12,62	-12,70	-12,71	-12,80
B1 + E	3,83	-4,73	-4,95	-4,89	-4,94	-4,88	-4,85
TS(B1 + B2)+E	5,27	-3,23	-3,46	-3,41	-3,46	-3,40	-3,36
B2 + E	-3,89	-10,18	-9,22	-9,19	-9,27	-9,27	-9,34
TS(B2 + B3)+E	-2,13	-8,33	-7,69	-7,66	-7,74	-7,73	-7,78
B3 + E	-4,58	-9,12	-8,20	-8,18	-8,26	-8,26	-8,34
TS(B3 + B4)+E	9,09	2,35	2,57	2,59	2,53	2,56	2,55
B4 + E	6,27	0,41	0,91	0,92	0,85	0,88	0,84
B5 + P + E	12,11	0,77	0,38	0,44	0,38	0,44	0,48

3.3. Monte Carlo classic simulation

Monte Carlo simulations provide important insight into the solvation of different chemical species; in our case, this information is essential to understanding the influence of the solvent on olefin metathesis because solvation plays a major role in the reaction yield. We began by analysing the solvation structure of the pre-catalyst **A1**. Radial distribution functions (RDF) show the probability of finding solvent molecules at a certain distance of the solute; a peak in the RDF indicates a layer of solvation. Generally, the RDF uses the distances between the centre-of-mass of the solute and each solvent molecule in the analysis [43]. This approach, however, is not as reliable for asymmetric solutes, as is the case for the pre-catalyst **A1**; therefore, we used distances between all atoms of the catalyst and all atoms of the solvent that were closest to the molecules (*Minimum Distance Function Distribution-MDDF*). This approach is widely used for the study of solvents with asymmetrical shapes [44]. The MDDF of water, water–methanol 3:1, water–methanol 1:1, water–methanol 1:3, methanol and dichloromethane are shown in Fig. 6.

For all solvents studied, the process of solvation had two major peaks or two layers of solvation. The first peak starts at approximately 1.1 Å, has a maximum at approximately 2.3 Å and ends at approximately 4.1 Å. These values obviously depend on the solvent, but these values represent the average for all solvents. The second peak starts at the end of the first, has its maximum at approximately 5.2 Å and ends at 8 Å. All solvents exhibit this distance behaviour except for dichloromethane whose peaks are farther from the catalyst. Table 4 shows the structural analysis of the solvation layers as well as the number of solvent molecules (N_{mol}) at each layer.

The number of molecules in each of the solvation layers decreases with an increasing proportion of methanol in the mixture, and among the solvents studied, dichloromethane had the lowest amount of solvating molecules. This decrease is because methanol molecules are larger than water, an explanation verified in other research [45]. Dichloromethane had less molecules than methanol not only because a dichloromethane molecule is bigger than methanol but also because it does not form hydrogen bonds with the solute.

We also analysed the solvation of the N-tosyldiallylamine (**O**) (Fig. 7) because the solubility of the olefin in the solvent is also important in the reaction yield [8]. Fig. 7 shows the MDDF of the

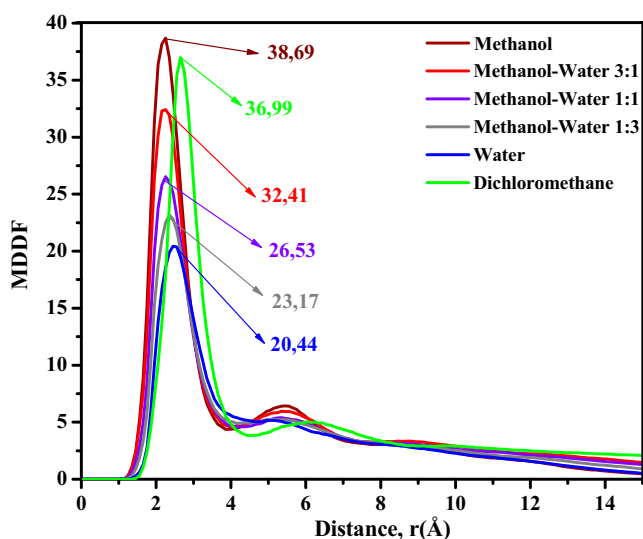


Fig. 6. MDDF between all atoms of the catalyst to all atoms of the solvent. Maximum peak value in evidence.

N-tosyldiallylamine in the same solvents studied for the catalyst. The structure of solvation is also characterised by two peaks for all solvents. The first peak, i.e., the first solvation layer, starts at approximately 1.5 Å, has a maximum at 2.5 Å and ends at 4.2 Å; the second peak begins at 4.2 Å, has its apex at approximately 5.2 Å and ends at 7.3 Å. Dichloromethane solvation also has two layers; however, the values of the radii to the beginning, apex and end of the solvation layers are greater. Fig. 6 summarise the number of water molecules present at the end of the first layer of solvation for each solvent. We found the same trend as shown by the catalyst: a reduced number of solvent molecules is present in the layers of solvation as the size of the solvent molecule increases.

A solvation process is better defined if it has more RDF peaks and more intense peaks. The MDDFs of the catalyst **A1** as well as those of the olefin, shown in Figs. 5 and 6, respectively, exhibit an increase in peak intensity as the number of low polarity molecules increases. For the catalyst, the peaks are largest with methanol and decrease somewhat with dichloromethane. The second peak nearly proportionally disappears as water content in the solution increased. This behaviour shows that non-polar solvents are better able to solvate the catalyst. The decrease in solvation by the dichloromethane is perhaps due to its inability to make hydrogen bonds. Better solvation allows for an interaction between the catalyst and the olefin, which favours the overall reaction. Methanol solvates the catalyst better than the dichloromethane, which explains the high yield of the reaction in methanol.

For N-tosyldiallylamine, the intensity of the peaks also follows the same trend as with the catalyst. The peaks are better defined as the solvent becomes more non-polar, and again, the second peak substantially disappears as the amount of water increases in the solution. The difference lies in the increased solvation by dichloromethane, whose peak corresponding to the first solvation layer is more intense than that of methanol. This is quite interesting because it shows that all of the olefin present in the reaction medium is soluble in dichloromethane. Therefore, dichloromethane best facilitates interaction between the catalyst and substrate, which is in agreement with the experimental results that suggested that dichloromethane is the best solvent among those considered here for the metathesis reaction, followed by methanol.

With the Monte Carlo simulation, we could not support the experimental results that show a high yield when using water as the solvent. These previous results showed that yield fell when adding 75% methanol but increased as the proportion of water was increased. Interestingly the high yield in methanol is only slightly higher than the yield in water. In our simulations, we found that water is the worst solvent, and yield improves as methanol is increased in the mixture. The simulation did confirm the experimental result that the dichloromethane is the best solvent. Certainly, other factors influence the experimental yield that need to be investigated, or maybe other methodologies could explore the influence of the solvent.

Based on the Monte Carlo simulations, we predicted trends for how the solvation process affects the behaviour of the radial distribution and the interactions between the solute and solvent. According to Table 5, these predictions are well-founded both for the catalyst **A1** as well as for N-tosyldiallylamine.

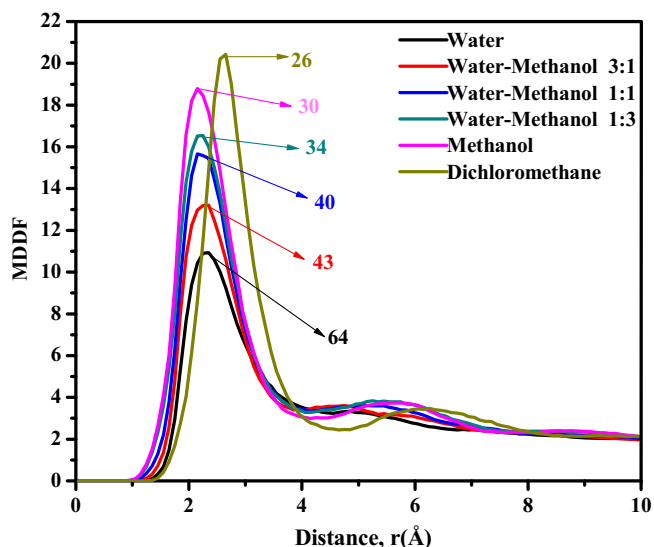
The interaction energy for the catalyst follows the same trend as the MDDFs. It becomes larger with increasing non-polar solvents in the medium, but it decreases for dichloromethane. Dichloromethane's interaction energy was again lower than methanol, which is likely due to its inability to make hydrogen bonds.

For N-tosyldiallylamine, the behaviour is again consistent, but the mixture of water–methanol 1/1 appears to have the highest interaction energy among the mixtures of methanol and water in disagreement with the MDDF results. The highest interaction

Table 4

Structure of layers of solvation of the Hoveyda-Grubbs catalyst, and various solvents, as well as the number of molecules in each layer of solvation.

Solvent	First Shell				Second Shell			
	Start	Max.	End	N_{mol}	Start	Max.	End	N_{mol}
Water	1,05	2,45	4,65	116	4,65	5,15	7,75	315
Water–Methanol 3/1	1,15	2,35	4,15	75	4,15	5,15	7,65	248
Water–Methanol 1/1	0,95	2,25	4,15	65	4,15	5,35	8,25	245
Water–Methanol 1/3	1,05	2,25	4,05	60	4,05	5,35	8,05	212
Methanol	1,15	2,25	3,85	54	3,85	5,45	7,65	172
Dichloromethane	1,45	2,65	4,45	41	4,45	6,05	8,75	133

**Fig. 7.** MDDF of solvation of N-tosyldiallylamine in different solvents and the number of molecules in the first solvation layer.**Table 5**Energy of interaction solute–solvent, in kcal mol⁻¹.

Solvent	Catalyst	N-tosyldiallylamine
Water	-79,81	-29,73
Water–Methanol 3/1	-83,30	-32,63
Water–Methanol 1/1	-84,93	-32,95
Water–Methanol 1/3	-88,43	-31,84
Methanol	-90,52	-33,04
Dichloromethane	-89,41	-33,24

energy is for dichloromethane, confirming that this solvent is the best solvent for the reaction, followed by methanol. Water, as expected, had the lowest interaction energy due to the hydrophobic character of the olefin.

4. Conclusions

In this research, we studied theoretically three aspects of the RCM of N-tosyldiallylamine using a Hoveyda–Grubbs catalyst:

- We investigated the whole catalytic cycle of the reaction in the gas phase, at the B3LYP/6–31 g (d)/LanL2DZ theoretical level and identified structures and energies that were in perfect agreement with previous studies. We also investigated two possible paths for the mechanism of initiation and found that the most favourable was the path that included an active species with 14 electrons (**A2**). This species undergoes an interconversion process without any energetic

barrier prior to the formation of a π -complex. Our olefin models might not have generated realistic results because our calculations indicate that π -complex formation is unfavourable using the real reactants (olefin and catalyst), which conflicts with the major literature. The energetic profile shown in gas phase suggests that the RCM reaction of the first olefin is less favourable than the entire catalytic cycle (19.21 and 12.11 kcal mol⁻¹, respectively).

- The influence of the solvent dielectric constant was studied via PCM, which resulted in more realistic energy values. The energy of coordination of the olefin **O** reduced. The π -complex that is formed after cycloreversion was no longer identified as an energy minimum. The reaction became more favourable overall. Formation of the first olefin was 19.21 kcal mol⁻¹ in the gas phase, while in dichloromethane, it became 13.67 kcal mol⁻¹. For the *turnover*, the energy was reduced from 12.11 to 0.48 kcal mol⁻¹. The PCM method did not show significant differences (relative to experimental error) between the different solvents, but it did suggest that the dichloromethane was the best solvent and that water was the worst. Mixtures of water/methanol showed almost the same values.
- The Monte Carlo simulations showed that both catalyst and olefin are solvated by two layers of solvents. It also showed that the dichloromethane is the best solvent for both the olefin and for the catalyst. Water is the solvent that has the least interaction with the catalyst and the olefin. As the proportion of methanol increased, so did the strength of the solvent–solute interaction, and therefore, the capacity of solvation. Finally, we found that pure methanol is the second best solvent of those we tested.

Acknowledgments

We would like to thank CAPES for the research grants, to Dr. Humberto Soares for computational support and Dr. Xavier Solans-Monfort for the discussions concerning the results of PCM. A major thanks to Dr. William Rocha, from UFMG, for his very important suggestion to this study and also for the computational support.

Appendix A. Supplementary material

Supplementary data associated with this article can be found, in the online version, at <http://dx.doi.org/10.1016/j.ica.2014.11.007>.

References

- [1] (a) J.M.E. Matos, N.C. Batista, R.M. Carvalho, S.A.A. Santana, P.N. Puzzi, M. Sanches, B.S. Lima-Neto, *Quim. Nova* 30 (2007) 431; (b) R.H. Grubbs, *Angew. Chem., Int. Ed.* 39 (2000) 3012.
- [2] F. Bernardi, A. Botoni, G.P. Miscione, *Organometallics* 22 (2003) 940.
- [3] J.C. Mol, *J. Mol. Catal. A: Chem.* 213 (2004) 39.

- [4] (a) I.C. Stewart, C.J. Douglas, R.H. Grubbs, *Org. Lett.* 10 (2008) 441;
(b) J.M. Berlin, S.D. Goldberg, R.H. Grubbs, *Angew. Chem., Int. Ed.* 45 (2006) 7591.
- [5] (a) C. Coperet, Beilstein J. Org. Chem. 7 (2011) 13;
(b) A.H. Hoveyda, S.J. Malcolmson, S.J. Meek, A.R. Zhugralin, *Angew. Chem., Int. Ed.* 49 (2010) 34;
(c) A. Aljarilla, J.C. Lopez, J. Plumet, *Eur. J. Org. Chem.* 32 (2010) 6123.
- [6] (a) J.-L. Hérisson, Y. Chauvin, *Makromol. Chem.* 141 (1971) 161;
(b) T.J. Katz, J. McGinnis, *J. Am. Chem. Soc.* 97 (1975) 1592.
- [7] (a) R.R. Schrock, *Chem. Rev.* 102 (2002) 145;
(b) G.C. Bazan, J.H. Oskam, H.-N. Cho, L.Y. Park, R.R. Schrock, *J. Am. Chem. Soc.* 113 (1991) 6899.
- [8] (a) S.T. Nguyen, R.H. Grubbs, *J. Am. Chem. Soc.* 115 (1993) 9858;
(b) P. Schwab, M.B. France, J.W. Ziller, R.H. Grubbs, *Angew. Chem., Int. Ed.* 34 (1995) 2039;
(c) T.M. Trnka, J.P. Morgan, R.H. Grubbs, *Tetrahedron Lett.* 40 (1999) 2247.
- [9] (a) J.S. Kingsbury, J.P.A. Harrity, P.J. Bonitatebus, A.H. Hoveyda, *J. Am. Chem. Soc.* 121 (1999) 791;
(b) S.B. Garber, J.S. Kingsbury, B.L. Gray, A.H. Hoveyda, *J. Am. Chem. Soc.* 122 (2000) 8168.
- [10] S. Gessler, S. Randl, S. Blechert, *Tetrahedron Lett.* 41 (2000) 9973.
- [11] S.H. Hong, R.H. Grubbs, *J. Am. Chem. Soc.* 128 (2006) 3508.
- [12] D. Burtscher, K. Grela, *Angew. Chem., Int. Ed.* 48 (2009) 442.
- [13] S.J. Connon, M. Rivard, M. Zaja, S. Blechert, *Adv. Synth. Catal.* 345 (2003) 572.
- [14] J.P. Gallivan, J.P. Jordan, R.H. Grubbs, *Tetrahedron Lett.* 46 (2005) 462577.
- [15] T.A. Kirkland, D.M. Lynn, R.H. Grubbs, *J. Org. Chem.* 63 (1998) 9904.
- [16] D.M. Lynn, B. Mohr, R.H. Grubbs, L.M. Henling, M.W. Day, *J. Am. Chem. Soc.* 122 (2000) 6601.
- [17] B. Mohr, D.M. Lynn, R.H. Grubbs, *Organometallics* 15 (1996) 4317.
- [18] X. Solans-Monfort, R. Pleixats, M. Sodupe, *Chem. Eur. J.* 16 (2010) 7331.
- [19] F. Nuñez-Zarur, X. Solans-Monfort, L. Rodríguez-Santiago, R. Pleixats, M. Sodupe, *Chem. Eur. J.* 17 (2011) 7506.
- [20] I.W. Ashworth, I.H. Hillier, D.J. Nelson, J.M. Percy, M.A. Vincent, *Chem. Commun.* 47 (2011) 5428.
- [21] T. Vorfalt, K.J. Wannowius, H. Plenio, *Angew. Chem., Int. Ed.* 49 (2010) 5533.
- [22] W. Kohn, L.J. Sham, *Phys. Rev.* 140 (1965) 1133.
- [23] A.D. Becke, *Phys. Rev. A* 38 (1988) 3098.
- [24] C. Lee, W. Yang, R.G. Parr, *Phys. Rev. B* 37 (1988) 785.
- [25] W.J. Hehre, R. Ditchfield, J.A. Pople, *J. Chem. Phys.* 56 (1972) 2257.
- [26] P.J. Hay, W.R. Wadt, *J. Chem. Phys.* 82 (1985) 270.
- [27] M. Cossi, V. Barone, R. Cammi, J. Tomasi, *Chem. Phys. Lett.* 255 (1996) 327.
- [28] P.S. Albright, L.J. Gosting, *J. Am. Chem. Soc.* 68 (1946) 1061.
- [29] V. Barone, M. Cossi, J. Tomasi, *J. Chem. Phys.* 107 (1997) 3210.
- [30] (a) A.A.C. Braga, G. Ujaque, F. Maseras, *Organometallics* 25 (2006) 3647;
(b) S. Kozuch, C. Amatore, A. Jutand, S. Shaik, *Organometallics* 24 (2005) 2319;
(c) J.M. Haynes, M. Viciano, E. Peris, G. Ujaque, A. Lledós, *Organometallics* 26 (2007) 6170.
- [31] (a) N. Bahri-Laleh, R. Credendino, L. Cavallo, Beilstein J. Org. Chem. 7 (2011) 40;
(b) S. Pandian, I.H. Hillier, M.A. Vincent, N.A. Burton, I.W. Ashworth, D.J. Nelson, J.M. Rinaubo, *G. Chem. Phys. Lett.* 476 (2009) 37.
- [32] A. Poater, F. Ragone, A. Correa, L. Cavallo, *Dalton Trans.* 40 (2011) 11066.
- [33] S.Z. Mikhail, W.R. Kimel, *J. Chem. Eng. Data* 6 (1961) 532.
- [34] C.M. Breneman, K.B.J. Wiberg, *Comput. Chem.* 11 (1990) 361.
- [35] (a) W.L. Jorgensen, D.S. Maxwell, J. Tirado-Rives, *J. Am. Chem. Soc.* 118 (1996) 11225;
(b) W.L. Jorgensen, BOSS, Version 4.6 Biochemical and Organic Simulation System User's Manual for UNIX, Linux, and Windows [Online], August, 2004, <<http://www.cemcomco.com/boss46.pdf>> (accessed November 11, 2012).
- [36] C.M. Aguillar, W.R. Rocha, *J. Phys. Chem. B* 115 (2011) 2030.
- [37] L.X. Dang, *J. Chem. Phys.* 110 (1999) 10113.
- [38] W.L. Jorgensen, *J. Phys. Chem.* 90 (1986) 1276.
- [39] W.L. Jorgensen, J. Chandrasekhar, J.D. Madura, R.W. Impey, M. Klein, *J. Chem. Phys.* 79 (1983) 926.
- [40] M.J. Frisch, G.W. Trucks, H.B. Schlegel, G.E. Scuseria, M.A. Robb, J.R. Cheeseman, G. Scalmani, V. Barone, B. Mennucci, G.A. Petersson, H. Nakatsuji, M. Caricato, X. Li, H.P. Hratchian, A.F. Izmaylov, J. Bloino, G. Zheng, J.L. Sonnenberg, M. Hada, M. Ehara, K. Toyota, R. Fukuda, J. Hasegawa, M. Ishida, T. Nakajima, Y. Honda, O. Kitao, H. Nakai, T. Vreven, J.A. Montgomery Jr., J.E. Peralta, F. Ogliaro, M. Bearpark, J.J. Heyd, E. Brothers, K.N. Kudin, V.N. Staroverov, R. Kobayashi, J. Normand, K. Raghavachari, A. Rendell, J.C. Burant, S.S. Iyengar, J. Tomasi, M. Cossi, N. Rega, J.M. Millam, M. Klene, J.E. Knox, J.B. Cross, V. Bakken, C. Adamo, J. Jaramillo, R. Gomperts, R.E. Stratmann, O. Yazyev, A.J. Austin, R. Cammi, C. Pomelli, J.W. Ochterski, R.L. Martin, K. Morokuma, V.G. Zakrzewski, G.A. Voth, P. Salvador, J.J. Dannenberg, S. Dapprich, A.D. Daniels, O. Farkas, J.B. Foresman, J.V. Ortiz, J. Cioslowski, D.J. Fox, Gaussian 09, Revision A.02, Gaussian Inc., Wallingford, CT, 2009.
- [41] F. Grisi, C. Costabile, E. Gallo, A. Mariconda, C. Tedesco, P. Longo, *Organometallics* 27 (2008) 4649–4656.
- [42] K. Coutinho, S. Canuto, DICE (v2.9): A Monte Carlo program for molecular liquid simulation, University of Sao Paulo, Brazil, 2003.
- [43] (a) S. Fomine, J.V. Ortega, M.A. Tlenkopathev, C. Adlhart, P. Chen, *J. Am. Chem. Soc.* 126 (2004) 3496;
(b) S.F. Vyboishchikov, M. Bühl, W. Thiel, *Chem. Eur. J.* 8 (2002) 3962.
- [44] (a) H.C. Georg, K. Coutinho, S. Canuto, *J. Chem. Phys.* 123 (2005) 124307;
(b) W.R. Rocha, V.M. Martins, K. Coutinho, S. Canuto, *Theor. Chem. Acc.* 108 (2002) 31.
- [45] (a) S. Canuto, K. Coutinho, D. Trzesniak, *Adv. Quantum Chem.* 41 (2002) 161;
(b) T. Andrade-Filho, H.S. Martins, J. Del Nero, *Theor. Chem. Acc.* 121 (2008) 147.